# Nanocrystalline mesoporous palladium activated tin oxide thin films as room-temperature hydrogen gas sensors†

**Goutam De,*[ab] Ralf Köhn,‡[b] George Xomeritakis[b] and C. Jeffrey Brinker*[bc]**

*Received (in Cambridge, UK) 2nd January 2007, Accepted 25th January 2007*
*First published as an Advance Article on the web 12th February 2007*
**DOI: 10.1039/b700029d**

**A unique nanocrystalline, mesoporous PdO–$SnO_2$ film exhibiting high sensitivity and selectivity to hydrogen gas at room temperature has been developed.**

$SnO_2$-based gas sensors work by monitoring changes in electrical resistance that result mainly from reduction/oxidation of the crystal surface by the target gas. To-date elevated temperatures[1–6] or UV light[7] are required to achieve rapid adsorption/desorption and oxidation/reduction kinetics needed for a practical, rapid, and sensitive $H_2$ detector. Very recently, nanocrystalline $SnO_2$-based sensors showed room temperature sensitivity towards ethanol and carbon monoxide, but poor sensitivity for hydrogen gas,[8,9] whereas indium oxide doped $SnO_2$ films deposited on microelectromechanical systems device showed an appreciable (but slow) response to $H_2$ gas at room temperature.[10] Here we are reporting a surfactant-templated unique nanocrystalline, mesoporous PdO–$SnO_2$ film exhibiting very high sensitivity and selectivity to hydrogen gas at room temperature. As hydrogen is currently used in many different sectors of technology and is expected to be the fuel of the future, a $H_2$-selective sensor material active at room temperature is of considerable immediate interest.[11]

Synthesis of mesoporous $SnO_2$ powders using cationic[6] or nonionic poly(ethylene oxide) based[12] surfactants has been recently reported. However, these methods are incapable of producing high quality films of $SnO_2$ or Pd-doped $SnO_2$, and to-date there are no reports of nanocrystalline mesoporous $SnO_2$ films having high surface area and room temperature gas sensitivity. We are reporting here a surfactant-directed assembly approach to form high surface area mesoporous Pd-doped $SnO_2$ films exhibiting an interconnected nanocrystalline structure and high sensitivity for $H_2$ gas at room temperature. We prepared uniform 8 mol% PdO–92 mol% $SnO_2$ (nominal composition) films on glass or Si-wafer substrates using the block copolymer surfactant Pluronic P123 ($PEO_{20}PPO_{70}PEO_{20}$) as a structure directing agent,[12] and tin (IV) *tert*-butoxide and Pd acetate as tin and palladium sources respectively (see experimental section in ESI†). To elucidate the role of nanostructuring, we also prepared films of identical composition without the surfactant. A main goal of our synthetic procedure was to incorporate Pd in $SnO_2$ as PdO, because, in this form, it is known to suppress grain growth in bulk sol–gel systems[13] and to increase both their on-set resistance value[3] and sensitivity towards $H_2$.[2,3] In addition, PdO acts as an electron acceptor, trapping charge from the $SnO_2$ conduction band. This trapped charge, along with that of ionosorbed oxygen, induces stronger depletion of electrons from the Sn oxide surface causing greater increases in resistance.[3] Films prepared with (molar ratio P123/Sn = 0.024) and without surfactant are designated $SnPd_S$ and $SnPd_\mathbf{0}$, respectively. The thickness of $SnPd_S$ film measured by ellipsometry and FE-SEM is about 230 nm. The FTIR spectrum of the $SnPd_S$ films dried at 100 °C showed C–H stretching vibrations associated with the surfactant. However, the spectrum of the corresponding air-annealed (400 °C/6 h) films showed complete removal of organics, having bands attributed solely to Sn–O (and possibly overlapped Pd-O) vibrations.[14] As prepared $SnPd_S$ films exhibited a broad low angle XRD peak (see Fig. S1 in ESI†) centered at $2\theta = 1.57°$ ($d$ = 5.62 nm), consistent with a worm-like micellar mesophase, whereas, as expected, the corresponding $SnPd_\mathbf{0}$ films showed no low angle X-ray diffraction. Upon calcination at 400 °C in air, $SnPd_S$ films crystallized, causing the low angle XRD peak to shift only slightly to lower $2\theta$ (larger *d*-spacing), reflective of the minor coarsening accompanying dimensionally-constrained framework crystallization. TEM imaging of calcined $SnPd_S$ films (Fig. 1) revealed a sponge-like morphology composed of uniform ~5 nm diameter grains (Fig. 1a), which is also confirmed by FE-SEM shown in the inset of Fig. 1a (top left). Energy dispersive X-ray scattering (Fig. 1b) confirmed the presence of Pd, Sn and O in the film. Selected area electron diffraction (SAED) patterns (inset of Fig. 1a) and wide angle XRD analyses (see Fig. S2 in ESI†) indicate a polycrystalline tetragonal structure (cassiterite), typical for $SnO_2$. The high-resolution electron micrograph (Fig. 1c) shows coalesced, almost spherical nanocrystalline grains with average diameters of 4–5 nm. Importantly, we could not locate any distinct PdO nanoparticles in FE-SEM or TEM investigations of the calcined films, and XPS analysis of the unsputtered film surface shows a Pd $3d_{5/2}$ line at 337.5 eV corresponding to the $Pd^{2+}$ ion.[15] These results imply that either a PdO–$SnO_2$ solid solutions formed,[16] or that PdO exists as extremely uniformly dispersed nanoparticles, but we could not distinguish between the two by wide-angle XRD.[17]

Surface acoustic wave-based nitrogen sorption analyses (at 77 K)[18] along with refractive index measurements were used to understand the influence of the templating procedure on thin film porosity (as opposed to the porosity of related mesoporous powders). Fig. 2a plots the nitrogen adsorption-desorption

---

[a] *Sol-Gel Division, Central Glass and Ceramic Research Institute, 196, Raja S.C. Mullick Road, Kolkata, 700 032, India.*
*E-mail: gde@cgcri.res.in; Fax: +91-33-24730957; Tel: +91-33-24838086*
[b] *Center for Micro-Engineered Materials, 203 Farris Engineering Center, University of New Mexico, Albuquerque, NM, 87131, USA*
[c] *Advanced Materials Laboratory, Sandia National Laboratories, 1001 University Blvd. SE, Suite 100, Albuquerque, NM, 87106, USA.*
*E-mail: cjbrink@sandia.gov; Fax: (505) 2727336; Tel: (505) 2727627*

† Electronic supplementary information (ESI) available: Experimental section and XRD results. See DOI: 10.1039/b700029d

‡ Present address: Department of Chemistry and Biochemistry, University of Munich, Butenandtstr. 5–13 (E), 81377 Munich, Germany.

This journal is © The Royal Society of Chemistry 2007

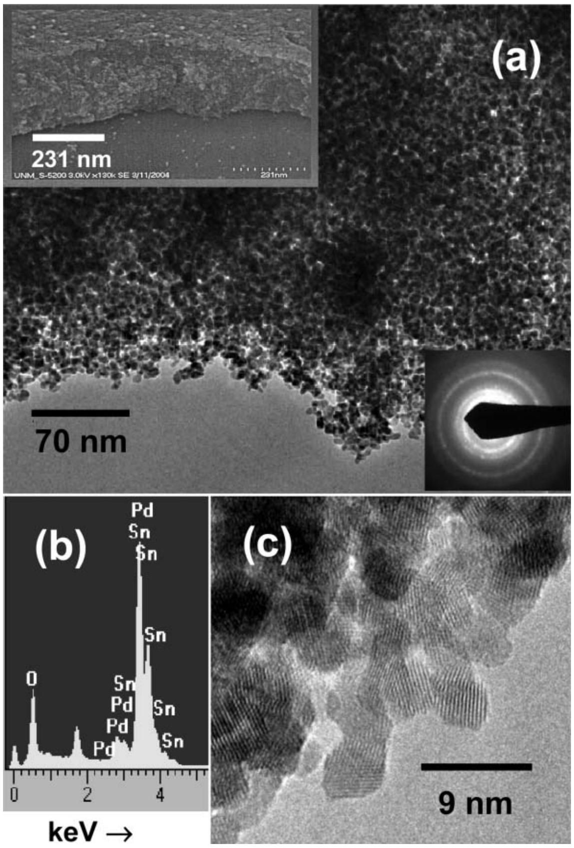

**Fig. 1** Electron microscopy images of $SnPd_S$ film calcined at 400 °C for 6 h in air. (a) Low magnification TEM image showing sponge-like porous structure of the film. Insets (top left) show the FE-SEM image taken at 40° tilt angle and selected area electron diffraction (SAED) pattern (below right) which could be indexed to tetragonal (cassiterite) $SnO_2$, (b) Energy dispersive X-ray scattering (EDX) taken from the above image showing presence of O, Pd and Sn and (c) High resolution TEM image showing lattice fringes corresponding to cassiterite $SnO_2$ of the near-spherical interconnected nanocrystals.

isotherms of the films prepared with and without surfactant. The $SnPd_0$ film prepared without surfactant has a low pore volume and surface area of 14.4 $m^2\ g^{-1}$ or 49.5 $m^2\ cm^{-3}$, compared to 143.5 $m^2\ g^{-1}$ or 493 $m^2\ cm^{-3}$ for the for the surfactant templated film $SnPd_S$. The pore size distribution of $SnPd_S$ is quite narrow, and the mean pore diameter, about 6.2 nm, is comparable to the nanocrystal diameter (Fig. 2b). The $SnPd_0$ film has a higher refractive index than the $SnPd_S$ film, 1.69 compared to 1.30, due to its much lower porosity. The measured surface area of the $SnPd_S$ film is quite high taking into account the high densities of the component oxides comprising the crystalline skeleton (6.95 and 8.3 g $cm^{-3}$ for $SnO_2$ and PdO, respectively), and comparable to reports of mesoporous $SnO_2$ powders prepared using surfactant templating.[12,19] There are no reports of corresponding nanocrystalline/high surface area $PdO/SnO_2$ films except for the case where trimethylsilyl termination of the surface hydroxyl groups was employed to avoid surface condensation reactions and, at high temperature, form silica nanoparticles that pin grain boundaries and suppress grain growth.[9] In our case, confinement within the nanodomains, established by the templating procedure, presumably serves to foster particle coalescence but limits 3D grain growth, allowing the formation of a highly porous, high surface area, doped oxide.

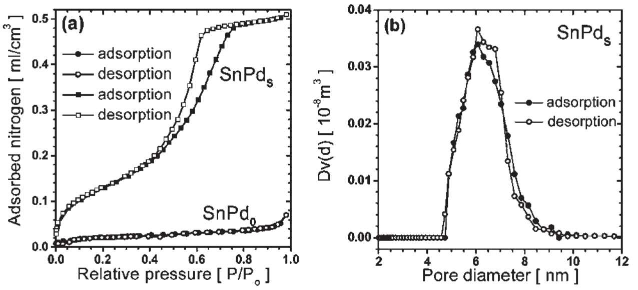

**Fig. 2** $N_2$ physisorption measurements at 77 K of the $SnPd_S$ and $SnPd_0$ films calcined at 400 °C for 6 h in air. (a) Nitrogen adsorption-desorption isotherms and (b) Pore size distributions of $SnPd_S$ film using density functional theory (DFT) method. The films were applied to ~1 $cm^2$ area of a piezoelectric ST-cut quartz SAW substrate with interdigitated gold transducers designed to operate at ~97 MHz. Mass change was monitored as a function of relative pressure (sensitivity ~80 pg $cm^{-2}$) using a surface acoustic wave (SAW) technique.[18]

Motivated by the high surface area and uniform incorporation of PdO within the $SnPd_S$ framework, gas sensing properties were measured at room temperature (21 ± 1 °C).[20] The sensor film has an initial resistance value of about 100–110 MΩ in air. Fig. 3a shows the decrease of the electrical resistance of the $SnPd_S$ film in

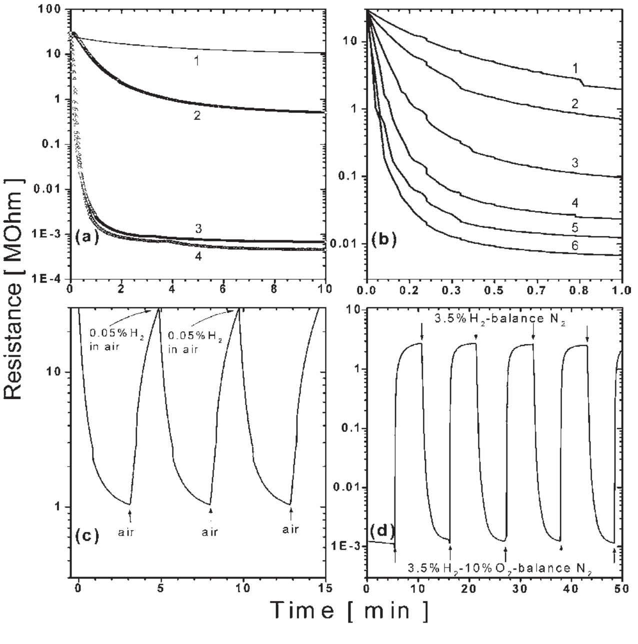

**Fig. 3** Gas sensing behaviour of $SnPd_S$ film at room temperature (21 ± 1 °C). The dynamic electrical responses (resistance range 30 MΩ and lower) to different gases was recorded with HP3478A digital multimeter using a LabView software (see ESI† for details). (a) Resistance changes when the sensor's surrounding atmosphere is switched from pure air to: (1) pure $CH_4$; (2) 0.5% vol. CO-in-$N_2$; (3) 0.5% vol. $H_2$-in-$N_2$; and (4) 0.5% vol. $H_2$-in-$N_2$, R.H. = 50%. (b) Resistance changes when the surrounding atmosphere is changed from pure air to: (1) 0.05% vol.; (2) 0.1% vol.; (3) 0.2% vol.; (4) 0.5% vol.; (5) 1.0% vol.; and (6) 2.0% vol. $H_2$-in-air. (c) Resistance changes when the sensor's surrounding atmosphere is cycled between air and 0.05% vol. $H_2$-in-air. (d) Cyclic resistance changes when 10% vol. $O_2$ is introduced or removed from a reducing process gas stream (here 3.5% vol. $H_2$-in-$N_2$).

response to pure $CH_4$ (1), 0.5% vol. CO-in-$N_2$ (2), 0.5% vol. $H_2$-in-$N_2$ (3) and humidified (R.H. = 50%) 0.5% vol. $H_2$-in-$N_2$ (4). The data indicate that the speed and magnitude of the response towards $H_2$ is much larger than the response to other reducing gases such as CO and $CH_4$. Also, the presence of $H_2O$ vapor in the surrounding atmosphere does not appear to interfere with the response towards $H_2$.

Fig. 3b shows the sensor's response towards increasing concentrations of hydrogen gas (0.05, 0.1, 0.2, 0.5, 1 and 2% vol.) in air. This response to different levels of $H_2$ in air is appreciably fast, especially as we approach the explosion limit of 4% vol. $H_2$-in-air. Fig. 3c shows reversible changes in resistance when the surrounding atmosphere is cycled between pure air and 0.05% vol. $H_2$-in-air, suggesting that the sensor responds very quickly to both the introduction as well as the removal of small amounts of $H_2$ gas in air. We have also tested the response to oxygen introduced in a hydrogen process stream by cycling the surrounding gas between the gas mixtures 3.5% $H_2$–balance $N_2$ and 3.5% $H_2$ −10% $O_2$–balance $N_2$. In this situation (Fig. 3d), the sensor's resistivity changes can alternatively be utilized as an alarm to signify the undesirable presence of $O_2$ (or its removal) in a reducing process gas stream.

The maximum gas sensitivity value $S$ (defined as the ratio of sensor resistance in air, $R_a$ to that in a sample gas, $R_g$)[3] of our sensor film ($SnPd_S$) was found to be about 300, 5000, and 20 000 for 0.05, 0.5 and 2% vol. $H_2$-in-air, and 100 000 for 0.5% vol. $H_2$-in-$N_2$, respectively. These values are very high ($\sim$3–4 orders of magnitude) in comparison to previously reported sensors operating at high (200–400 °C)[2–6] and low temperatures.[21] Moreover, our sensor's response to $H_2$ in air is also very fast for practical rapid detection of $H_2$. Beyond room temperature operation, another advantage of this sensor is that it is relatively insensitive to CO or $CH_4$, especially in the presence of $O_2$ (*e.g.* the sensor's sensitivity towards 0.05% vol. $H_2$ in air is 300-fold larger than towards 0.05% vol. CO in air).

It has been reported that reduced grain size could enhance the sensitivity of $SnO_2$[9] towards reducing gases. The unusually high hydrogen sensitivity and rapid response of our films at room temperature presumably results from the high surface area, 3-D accessible sponge-like mesoporous structure, and uniform incorporation of PdO in the $SnO_2$ lattice. The surfaces of the interconnected nanosized single crystalline grains of PdO–$SnO_2$ allow rapid room temperature reduction of $SnO_2$ in response to $H_2$, causing a dramatic decrease of resistance values. When the film is exposed to air (oxygen), the reduced film surface reverts back to its original state. This surface reduction/oxidation process proceeds with no measurable changes in lattice spacing or nanostructure of the $SnO_2$. In the case of CO or $CH_4$, the film shows much weaker room temperature sensitivity, as a result of the weak interaction of CO gas with $Pd^{2+}$ and $Sn^{4+}$ ions at room temperature[13,14] and the much weaker reducing character of $CH_4$ gas. On the other hand, $H_2O$ vapor only physisorbs on the $SnO_2$ surface at $T < 100$ °C with practically no[22] or very little effect on sensor's electrical resistance.[23]

In conclusion, we have demonstrated a synthesis approach that combines nanostructuring, molecular-level dispersion of a Pd catalyst, and homogenous film formation in a simple 'one-pot' process, leading to a unique material that overcomes existing barriers to rapid room temperature hydrogen detection by tin oxide. As an example, alternating between air and 0.5% vol. $H_2$ gas in $N_2$, changes the resistance reversibly and rapidly by a factor of about $10^5$ at room temperature. An additional advantage of this material is its relative insensitivity to other combustible gases such as CO or $CH_4$, or to ubiquitous $H_2O$ vapour.

The CSIR, India is thankfully acknowledged for awarding a '*Raman Research Fellowship*' to G. De for carrying out this work at UNM/AML/Sandia. Funding from Alexander von Humboldt Foundation, DOEBES, NSF, AFOSR, ARO and NASA is thankfully acknowledged. Sandia is a Multiprogram laboratory operated by Sandia Corporation, a Lockheed-Martin Company, for the United States Department of Energy's National Nuclear Security Administration under Contract DE-AC04-94AL85000.

## Notes and references

1 K. Ihokura and J. Watson, *The Stannic oxide Gas Sensor: Principles and Applications*, CRC Press, Boca Raton, FL, 1994.
2 G. De, A. Licciulli, C. Massaro, A. Quirini, R. Rella, P. Siciliano and L. Vasanelli, *Sens. Actuators, B*, 1999, **55**, 134; A. Licciulli, S. Mazzarelli, G. De, P. Siciliano, L. Vasanelli and R. Rella, *J. Sol-Gel Sci. Technol.*, 2001, **21**, 195.
3 N. Yamazoe, *Sens. Actuators, B*, 1991, **5**, 7.
4 N. Bârsan, J. R. Stetter, M. Findlay, Jr. and W. Göpel, *Anal. Chem.*, 1999, **71**, 2512.
5 Z. L. Wang, *Adv. Mater.*, 2003, **15**, 432.
6 T. Hyodo, S. Abe, Y. Shimizu and M. Egashira, *Sens. Actuators, B*, 2003, **93**, 590.
7 P. Camagni, G. Faglia, P. Galinetto, C. Perego, G. Samoggia and G. Sberveglieri, *Sens. Actuators, B*, 1996, **31**, 99.
8 Y. Wang, X. Jiang and Y. Xia, *J. Am. Chem. Soc.*, 2003, **125**, 16176.
9 N.-L. Wu, S.-Y. Wang and I. A. Rusakova, *Science*, 1999, **285**, 1375.
10 S. Shukla, P. Zhang, H. J. Cho, Z. Rahman, C. Drake and S. Seal, *J. Appl. Phys.*, 2005, **98**, 104306.
11 F. Favier, E. C. Walter, M. P. Zach, T. Benter and R. M. Penner, *Science*, 2001, **293**, 2227.
12 P. Yang, D. Zhao, D. I. Margolese, B. F. Chmelka and G. D. Stucky, *Chem. Mater.*, 1999, **11**, 2813.
13 T. Takeguchi, O. Takeoh, S. Aoyama, J. Ueda, R. Kikuchi and K. Eguchi, *Appl. Catal., A*, 2003, **252**, 205.
14 D. Amalric-Popescu and F. Bozon-Verduraz, *Catal. Today*, 2001, **70**, 139.
15 C. D. Wagner, A. V. Naumkin, A. K. Vass, J. W. Allison, C. J. Powell and J. R. Rumble, Jr., *NIST X-ray Photoelectron Spectroscopy data base 20*, vers. 3.4, August 2003.
16 J. Han and S. Hong, *Jap. J. Appl. Phys.*, 2005, **44**, 7698.
17 If a Pd atom substitutes a Sn atom in the tetragonal $SnO_2$ lattice (space group $P4_2$/mnm), there will be a 4% change in the lattice size, as a result of the shorter Pd–O bond distance (2.02 Å) compared to the Sn–O bond (2.10 Å). Overall there will be about 0.3% change in lattice size for 8 mol% substitution of Sn by Pd in the lattice. In this case, there will be only a 0.1° shift in the $2\theta$ angle of the most intense (110) reflection of tin oxide, which cannot be detected due to the broad peaks of our nanocrystalline thin film sensor. On the other hand, if PdO exists as discrete nanoparticles, it would be hard to detect it with wide-angle XRD since its most intense peaks, (101) and (002), coincide with the (101) peak of $SnO_2$.
18 Y. Lu, R. Ganguli, C. A. Drewien, M. T. Anderson, C. J. Brinker, W. Gong, Y. Guo, H. Soyez, B. Dunn, M. H. Huang and J. I. Zink, *Nature*, 1997, **389**, 364.
19 T. Katou, D. Lu, J. N. Kondo and K. Domen, *J. Mater. Chem.*, 2002, **12**, 1480.
20 The $SnPd_0$ film prepared without surfactant showed negligible response towards $H_2$ gas at room temperature.
21 J. Gong, Q. Chen, W. Fei and S. Seal, *Sens. Actuators B*, 2004, **102**, 117.
22 N. Bârsan and U. Weimer, *J. Electroceram.*, 2001, **7**, 143.
23 G. Korotchenkov, V. Brynzari and S. Dmitriev, *Sens. Actuators, B*, 1999, **54**, 197.

Supplementary Material (ESI) for Chemical Communications
This journal is (c) The Royal Society of Chemistry 2007

# Nanocrystalline mesoporous palladium activated tin oxide thin films as room-temperature hydrogen gas sensors†

**Goutam De,*[a,b] Ralf Köhn,[b+] George Xomeritakis[b] and C. Jeffrey Brinker*[b,c]**

**Manuscript no. B700029D**

## Electronic supplementary information (ESI)

### Experimental:

All chemicals were used as received. Tin (IV) tert-butoxide ($Sn(OBu^t)_4$), palladium acetate ($Pd(CH_3COO)_2$) and solvents (*n*-propanol and i-butanol) were obtained from Aldrich, while the acetic acid was supplied by J.T. Baker. The surfactant Pluronic P123 was donated by BASF Corporation. Compressed gas mixtures of 0.5% vol. $H_2$-in-$N_2$, 0.5% vol. CO-in-$N_2$, forming gas (7% vol. $H_2$-in-$N_2$), $N_2$, $CH_4$ and compressed air were obtained from Matheson Tri-Gas.

*Preparation of sols*

2.43 mmol $Sn(OBu^t)_4$ was first dissolved in 12.3 mmol *n*-propanol. To this 0.0583 mmol surfactant dissolved in 16.4 mmol *n*-propanol was added with stirring. A mixture of 9.72 mmol acetic acid in 12.3 mmol *n*-propanol, followed by 14.2 mmol *i*-butanol was added to the above solution with stirring. The stirring was continued overnight (16 h). 0.211 mmol $Pd(CH_3COO)_2$ was dissolved in 22 mmol acetone and added to the above sol with stirring. The doped sol is then filtered through a 0.2 μm GHP Acrodisc® membrane

This journal is (c) The Royal Society of Chemistry 2007

(Gelman Laboratory) prior to use for coating depositions. For comparison, a PdO-$SnO_2$ film without surfactant was also prepared. The nominal oxide molar ratio $SnO_2$:PdO = 92:8 was maintained in the sols. The total oxide ($SnO_2$ + PdO) equivalent content in the sols was about 5.8% wt. in all cases.

*Preparation of films*

Homogeneous films were deposited on plasma cleaned silicon wafers, Corning 7059, and silica glass substrates by spin-coating under ambient conditions (room temperature 21±1°C, relative humidity 5-10%), employing a spinning rate of 1,800 rpm. The films were stored in plastic boxes overnight and then dried at 100°C in air. The resulting dried films were then calcined for 6 h at 400°C in air.

*Characterization*

Refractive index and thickness measurements were made with a J.A. Wollam Co. M44 spectroscopic ellipsometer. All refractive index values (reported at a wavelength of 630.5 nm) and thickness measurements were made in triplicate and averaged. FTIR spectra were taken on a Bruker spectrometer (model Vector 22). XRD was recorded on a Siemens D-500 diffractometer, using a Cu $K_\alpha$ source. TEM was performed on a JEOL 2010 microscope, equipped with an energy dispersive X-ray scattering measurement (EDX) facility. High resolution SEM (FE-SEM) images were obtained in a Hitachi field-emission scanning electron microscope. X-ray photoelectron spectra (XPS) were obtained in a Kratos Axis Ultra XPS using a monochromatic Al $K_\alpha$ X-ray source.

*Gas Sensing Measurements*

For gas sensing measurements, the films were deposited on SAW substrates. The sensor film was sealed with copper O-ring inside a custom stainless steel holder, having appropriate electrical contacts with the two gold electrodes of the SAW device substrate, and equipped with inlets and outlets for gas flow. A mixture of air, 0.5% vol. $H_2$-in-$N_2$, 0.5% vol. CO-in-$N_2$, forming gas (7% vol. $H_2$–in-$N_2$), $CH_4$ and $N_2$ was flown over the sensor at a fixed total flow rate of 100 SCCM and $P_{tot} = 1$ atm, adjusted with the aid of 2 mass flow controllers (Brooks Instr.). The gas relative humidity (R.H.) was controlled by flowing part of the gas through a bubbler filled with DI water. The film’s electrical response (resistance range of 30 MΩ and lower) to different gases was recorded with a Hewlett Packard 3478A digital multimeter connected with a computer for data acquisition using LabView software. All dynamic resistance measurements are therefore reported from 30 MΩ to lower values and the data points are collected in every 1 sec of interval. A Techtron® DT-20 multimeter was used to record film resistances manually above 30 MΩ.

**Electronic Supplementary Information (XRD results)**

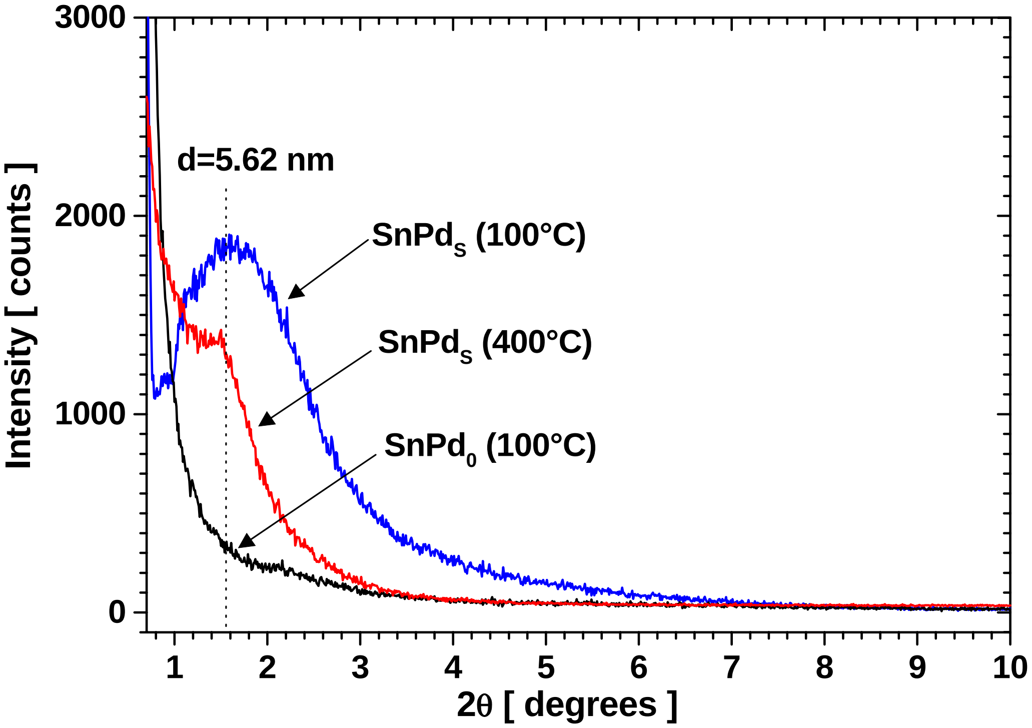

**Fig. S1.** Low angle XRD of SnPd$_S$ films deposited on Corning 7059 glass substrates. The low angle XRD of the corresponding SnPd$_0$ film prepared without surfactant is also shown.

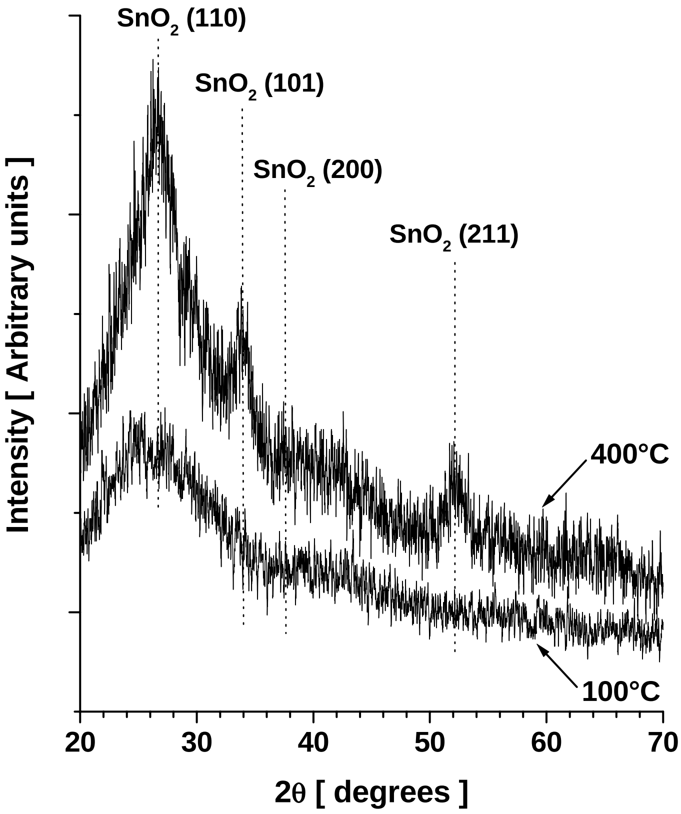

**Fig. S2.** The wide angle XRD of $SnPd_S$ films deposited on Corning 7059 glass substrates heated at 100 and 400 °C. The 400 °C film shows broad peaks corresponding to cassiterite $SnO_2$ structure. The $SnO_2$ (101) peak overlaps with broad amorphous peak arising from the glass substrate.